

# Conductivity and structure features of $\text{Ce}_{1-x}\text{Gd}_x\text{O}_{2-\delta}$ solid electrolytes fabricated by compaction and sintering of weakly agglomerated nanopowders

V.V. Ivanov\*, V.R. Khrustov, Yu.A. Kotov, A.I. Medvedev,  
A.M. Murzakaev, S.N. Shkerin, A.V. Nikonov

*Institute of Electrophysics, UD RAS, 106, Amundsen Str., Ekaterinburg 620016, Russia*

Available online 19 June 2006

## Abstract

The conductivity and structure features of  $\text{Ce}_{1-x}\text{Gd}_x\text{O}_{2-\delta}$  ceramics prepared using weakly agglomerated nanopowders with the average particle size of about of 15 nm are discussed. The powders were synthesized by the evaporation of coarse-grained target with the use of pulsed  $\text{CO}_2$ -laser radiation. The magnetic pulsed compaction method was applied to press a dry nanopowder to densities up to 55% of theoretical one. Owing to high activity of the starting powder and uniformity of the compacts, the sintering of ceramics up to near full density was realized in non-conventionally low temperature range of 1100–1300 °C. The structure of sintered ceramics with average grain sizes from the range of 100–300 nm was investigated by X-ray analysis and microscopy methods (AFM, SEM). The structure features are discussed in interrelation with the data on conductivity of ceramics. The significant deviation in lattice parameter of elementary cubic cell for sintered fine-grained ceramics as compared with the known data for conventional coarse-grained material was revealed.

© 2006 Elsevier Ltd. All rights reserved.

**Keywords:** Sintering; Nanopowders;  $\text{CeO}_2$ ; Electrical conductivity; Grain size

## 1. Introduction

The Gd-doped ceria solid solutions have been regarded as the promising electrolytes for the intermediate temperature (500–800 °C) solid oxide fuel cells (SOFC)<sup>1,2</sup> due to enhanced oxygen-ion conductivity compared to zirconia solid solutions. Methods of fabricating and properties of these electrolytes are actively studied.<sup>1–8</sup> However, conventional micron-sized powdered  $\text{CeO}_2$ -based materials are difficult to densify, even sintered at higher temperatures for a long time.<sup>3,4</sup> Higher sintering temperatures lead to a high manufacture cost for SOFC systems because ceria-based electrolyte and other components such as electrodes, cannot be cofired at temperatures higher than 1300 °C.

Moreover, the high efficiency of SOFC devices is expected at electrolyte layers of the micron scale thickness. In this connection the fabrication and properties study of  $\text{Ce}_{1-x}\text{Gd}_x\text{O}_{2-\delta}$

solid solutions with near full density and fine structure of submicron- and nano-sized range is of great interest. In order to reduce sintering temperatures and get ceria solid solutions with submicron microstructure, the nano-sized powders with a high sintering activity should be used. Quality of a starting nanopowder (particle size distribution, impurities, additives, etc.) effects essentially on electrochemical and mechanical properties of sintered ceramics. Considerable changes in the transport properties in such solid electrolytes could be expected upon reducing the average grain size of crystallites to a submicron range (0.1–1  $\mu\text{m}$ ). The fine-grained solid electrolytes possess a developed intercrystalline boundary, whose properties are likely to substantially affect the charge transport.

The aim of the present paper is to examine the sintering behavior of weakly agglomerated nano-sized powders  $\text{Ce}_{1-x}\text{Gd}_x\text{O}_{2-\delta}$  prepared by the laser evaporation method. Also, the results on the influence of the microstructure (on submicron scale), density and composition ( $x=0.09\text{--}0.31$ ) of the sintered solid electrolytes on ionic conductivity are presented.

\* Corresponding author. Tel.: +7 343 2678775; fax: +7 343 2678794.  
E-mail address: [ivanov@iep.uran.ru](mailto:ivanov@iep.uran.ru) (V.V. Ivanov).

## 2. Experimental

### 2.1. Preparation of nano-sized powders

The nano-sized powders of ceramics  $\text{Ce}_{1-x}\text{Gd}_x\text{O}_{2-\delta}$  with a variable molar fraction  $x$  of gadolinium ( $x=0.09\text{--}0.31$ ) were prepared by a method of a laser evaporation of a target (LEC) using the radiation of a  $\text{CO}_2$  laser.<sup>9</sup> The mixtures of preliminarily certified coarse powders of micron dimensions were used to fabricate targets for the laser evaporation.<sup>10</sup> After the laser synthesis, the powders were sedimented in isopropanol in order to remove coarse particles with a size exceeding 200 nm. The most important property of these powders is a weak agglomeration of particles when dried. The available agglomerates in this case were easily broken down by an ultrasonic treatment upon a secondary deployment in the isopropanol. The composition of solid solutions of the synthesized powders was controlled by an elemental analysis (Jobin Yvon 48). The specific surface area of nano-sized powders of all compositions was approximately identical and amounted to  $56\text{ m}^2/\text{g}$ . With the aid of an X-ray diffraction analysis (XRD) with filtered  $\text{Cu K}\alpha$  radiation it was established, that the synthesized nanopowders of  $\text{Ce}_{1-x}\text{Gd}_x\text{O}_{2-\delta}$  ( $x=0.09\text{--}0.31$ ) are single-phased solid solutions with a cubic fluorite-like lattice type (e.g., lattice parameter  $a=0.5424\text{ nm}$  at  $x=0.20$ ). The average dimensions of crystallites determined by the Scherrer method using the broadening of the X-ray diffraction lines were about of  $d_x=19\text{ nm}$ . The grain strains were neglected here.

The nanopowder particles as can be seen from the character TEM image (Fig. 1), possess predominantly the form of a sphere. The distribution of particles by size is narrow and characterized with average geometrical diameter of particles  $d_g=9.4\text{ nm}$  at the magnitude of dispersion 1.7 (Fig. 2). As the average size of particles  $d_g$  happens to be considerably smaller than the average size of crystallites  $d_x$ , it is possible to conclude that particles of a powder are predominantly single crystals and free of strains.

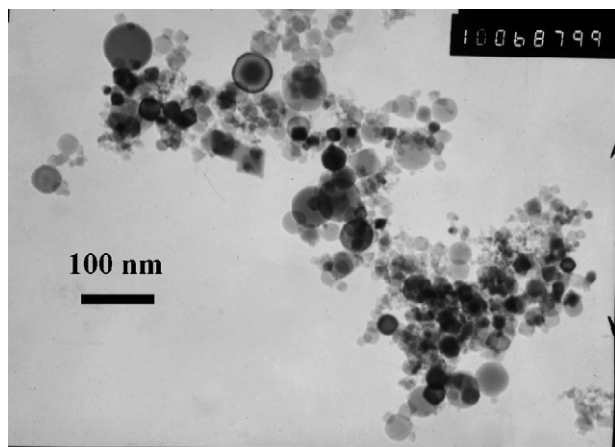


Fig. 1. The appearance of particles of  $\text{Ce}_{0.8}\text{Gd}_{0.2}\text{O}_{2-\delta}$  nanopowder under an electron microscope.

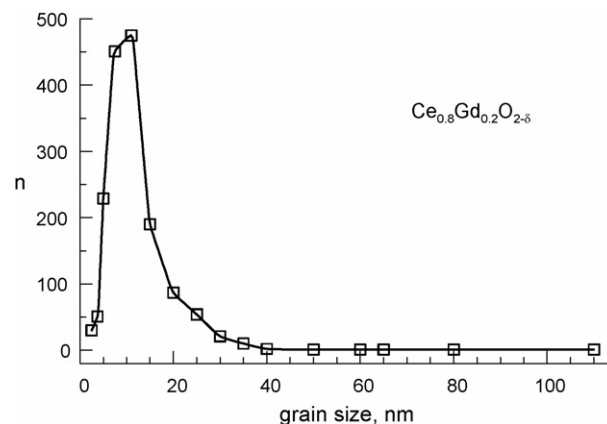


Fig. 2. The distribution of particles of  $\text{Ce}_{0.8}\text{Gd}_{0.2}\text{O}_{2-\delta}$  ceramics by size.

### 2.2. Preparation and characterization of ceramics

The synthesized powders were pressed in the form of a disk 30 mm in diameter and 2 mm thick by a magnetic pulsed compaction<sup>11</sup> at a pressure of 200 MPa to densities up to 55% of theoretical one. The theoretical density was calculated assuming the lattice parameter measured by X-ray analysis. Essentially, we conducted a dry pressing of powders, without using any binder. The pressed samples were sintered in air in an electric furnace at the temperature range of  $1100\text{--}1300^\circ\text{C}$  with heating and cooling rates of  $2^\circ\text{C}/\text{min}$ . The densities of the samples were determined by an Archimedes method with water.

The microstructure of the sintered ceramics with average grain sizes from the submicron range was investigated by X-ray analysis, AFM (Solver 47p) and SEM (LEO 982) microscopy methods. The mean grain size was calculated from AFM and SEM micrographs using the linear intercept technique.

### 2.3. Electrical characterization

Four-point conductivity measurements have been carried out on dense sintered test bars of  $20\text{ mm} \times 3\text{ mm} \times 1.5\text{ mm}$

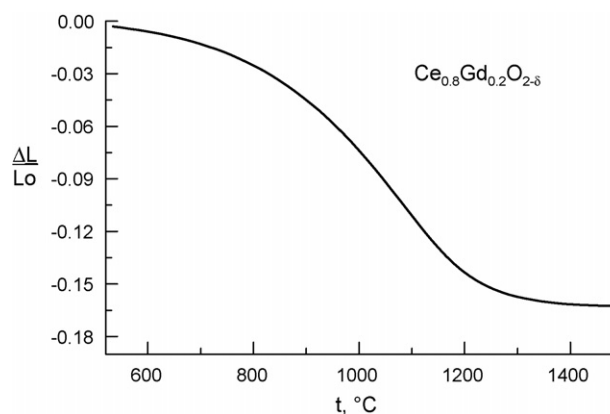


Fig. 3. Typical shrinkage-temperature curve for compact of  $\text{Ce}_{0.8}\text{Gd}_{0.2}\text{O}_{2-\delta}$  nanopowder.

(length  $\times$  width  $\times$  height) dimensions contacted by applying platinum paste and fixing platinum wires with ceramic binder. Measurements were taken in air in the temperature interval 500–900 °C with steps of 50° after holding time of 2 h at a temperature of test. The automotive testing facility with computer controlling was used that guarantees the relative error in the measurements well below 0.5–1%. The error in the measurements of the  $I/s$  ratio of samples was equal to 1–2%.

AC two-probe impedance spectroscopy was performed on thin plate 0.5 mm thick of  $\text{Ce}_{0.8}\text{Gd}_{0.2}\text{O}_{2-\delta}$  ceramics. Large opposite surfaces had silver electrodes, which were fused at

700 °C for nearly 18 h. The measurements were carried out in air over a temperature interval of 220–700 °C with steps of 20–50° using a Zahner FRA (IM6, Zahner, Germany) in the frequency range  $10^{-1}$  to  $8 \times 10^5$  Hz.

### 3. Results and discussion

The sintering behavior of the powdered compacts has been investigated in dilatometer with heating rate of 5 °C/min at the temperatures up to 1500 °C. As can be seen from the character shrinkage–temperature curve (Fig. 3) the active shrinkage of compacts starts near 600 °C and finishes approximately at

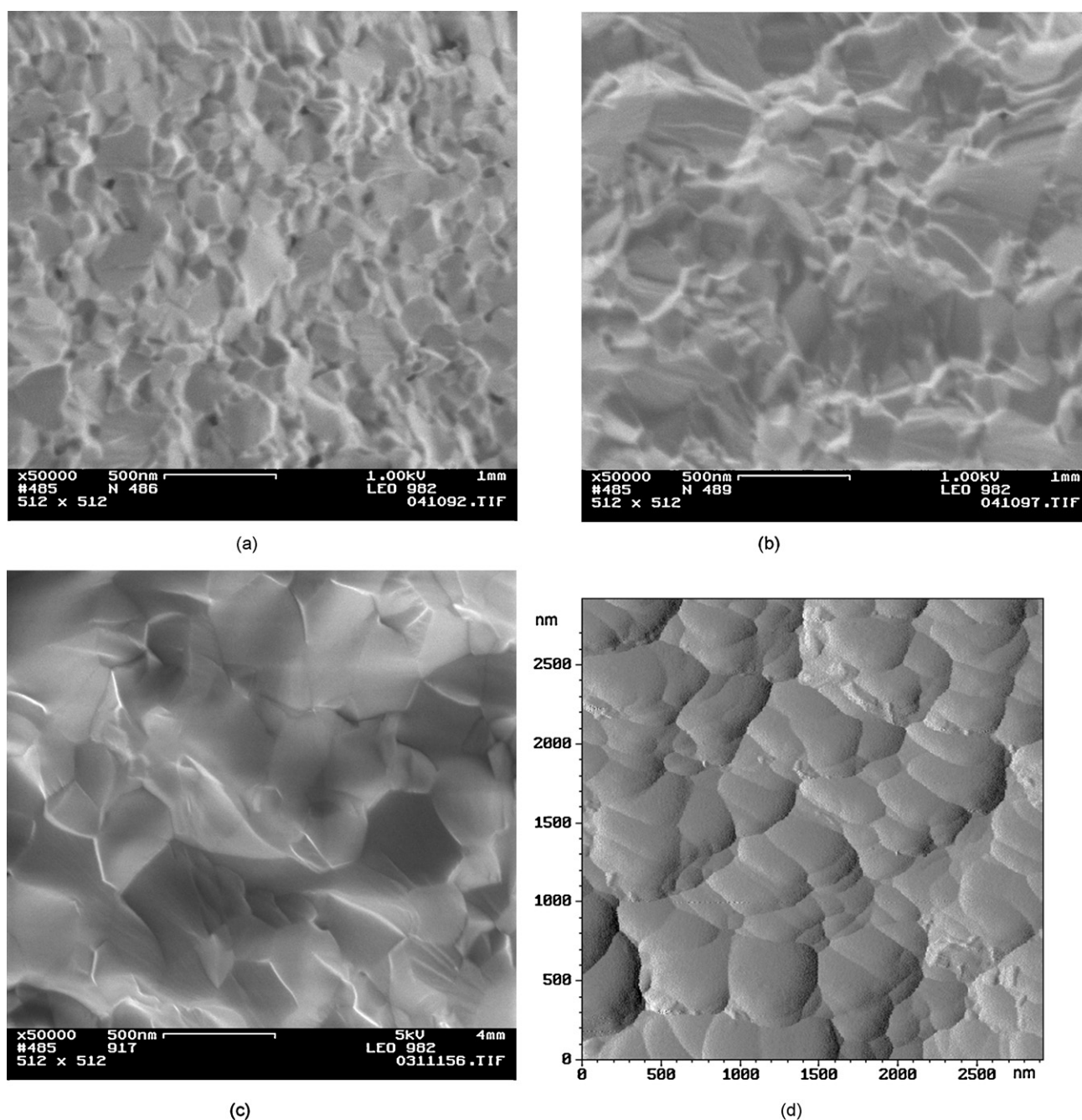


Fig. 4. The appearance of samples of ceramics of the composition  $\text{Ce}_{0.8}\text{Gd}_{0.2}\text{O}_{2-\delta}$ : (a) sintering at 1100 °C, relative density 0.94 (LEO 982); (b) sintering at 1200 °C, relative density 0.98 (LEO 982); (c) sintering at 1300 °C, relative density 1.00 (LEO 982); (d) sintering at 1100 °C with a 108 h exposure, relative density 0.99 (ASM).

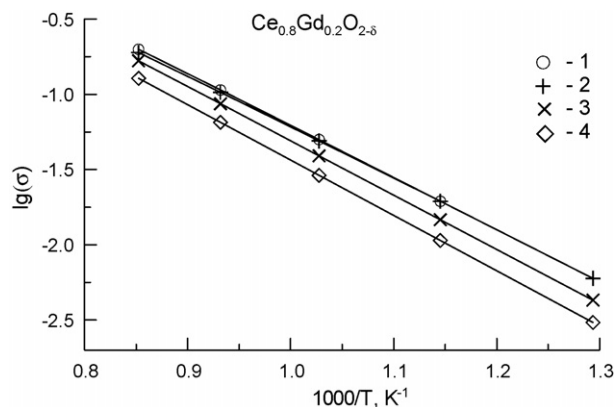


Fig. 5. The temperature dependences of total electrical conductivities of  $\text{Ce}_{0.8}\text{Gd}_{0.2}\text{O}_{2-\delta}$  ceramics sintered at different modes (Table 1).

1200 °C. So fast sintering is indicative for the low agglomeration and high sintering activity of synthesized nanopowder.

We compared the results of measurements of the electroconductivity of samples of solid electrolytes  $\text{Ce}_{0.8}\text{Gd}_{0.2}\text{O}_{2-\delta}$  with different densities and mean grain size, which were sintered from identical compacts at various temperatures, holding time modes. An analysis of the microstructure of the ceramics showed that, once the sintering temperature  $T_s$  was elevated in the region of 1100–1300 °C at zero holding time, the average size of grains in a material increased from approximately 100–300 nm at the density increase from 0.94 to 1.0 of theoretical one. In particular, the photographs presented in Fig. 4a–c give a comparison of microstructures of the samples of the  $\text{Ce}_{1-x}\text{Gd}_x\text{O}_{2-\delta}$  ceramics with the gadolinium fraction  $x=0.2$ , which had been sintered at different temperatures. Pores of diverse angular forms the size of a few tens of nanometers at the grain joints are characteristic of the microstructure of a ceramics sintered at a temperature of 1100 °C (Fig. 4a). Upon an increase in the sintering temperature, the pores diminish and lines of growth are observed at the surface of grains (Fig. 4b). Following an increase in the sintering temperature to 1300 °C, the grains acquired a clear-cut faceted form (Fig. 4c). No differences in the microstructure of samples of ceramics with different contents of gadolinium ( $x=0.09$ –0.31) were found.

Moreover, the long holding time  $t_s$  can lead to near full densification with minor grain growth at essentially low sintering temperature  $T_s$ . This behavior illustrates with image in Fig. 4d for the ceria sample sintered at  $T_s=1100$  °C with holding for  $t_s=108$  h. The estimated mean grain size of it is equal to 220 nm.

Shown in Fig. 5 are the Arrhenius plots of total electrical conductivities of  $\text{Ce}_{0.8}\text{Gd}_{0.2}\text{O}_{2-\delta}$  ceramics sintered at different modes collected in Table 1. It is observed that the highest conductivity values correspond to the samples with the largest densities (1 and 2), and otherwise the lower a density the worse a conductivity. From conductivity results the activation energy  $E_a$  was derived. These values ranging from 0.76 to 0.81 eV are typical for well-sintered ceramics reported in the literature.<sup>1</sup> It is worth to emphasize the slight increase in  $E_a$  with density diminishing, too. At the same time there are no correlations between the total electrolyte conductivity and sintering temperature or mean

Table 1

Characteristics of  $\text{Ce}_{0.8}\text{Gd}_{0.2}\text{O}_{2-\delta}$  samples with various densities, which obey different conductivities as shown in Fig. 5

	Sample no.			
	1	2	3	4
Relative density	1.00	0.99	0.98	0.94
$d$ (nm)	300	220	190	90
$E_a$ (eV)	0.77	0.76	0.80	0.81
$T_s$ (°C)	1300	1100	1200	1100
$t_s$ (h)	0	108	0	0

grain size  $d$  measured from SEM and AFM images. This could be attributed to essential role of ceramics density at good quality of grain boundaries in forming conditions for conductivity.

The impedance spectroscopy measurements allowed separating contributions from electrode processes ( $R_\eta$ ), resistance of the grain bulk ( $R_{\text{bulk}}$ ), and resistance of grain boundaries ( $R_{\text{gb}}$ ) in a  $\text{Ce}_{0.8}\text{Gd}_{0.2}\text{O}_{2-\delta}$  ceramics with near full density. Fig. 6a presents typical hodograph curves of the cell impedance for plate-like sample. Its total electroconductivity in comparison with contributions of the grain bulk and grain boundaries conductivities is shown in Fig. 6b. It is commonly assumed that the main reason for the decrease in the total electroconductivity of ceramics is grain boundaries and impurities, primarily Si, localized at boundaries. Notice that although the share of grain boundaries in the material, which was sintered from nanopow-

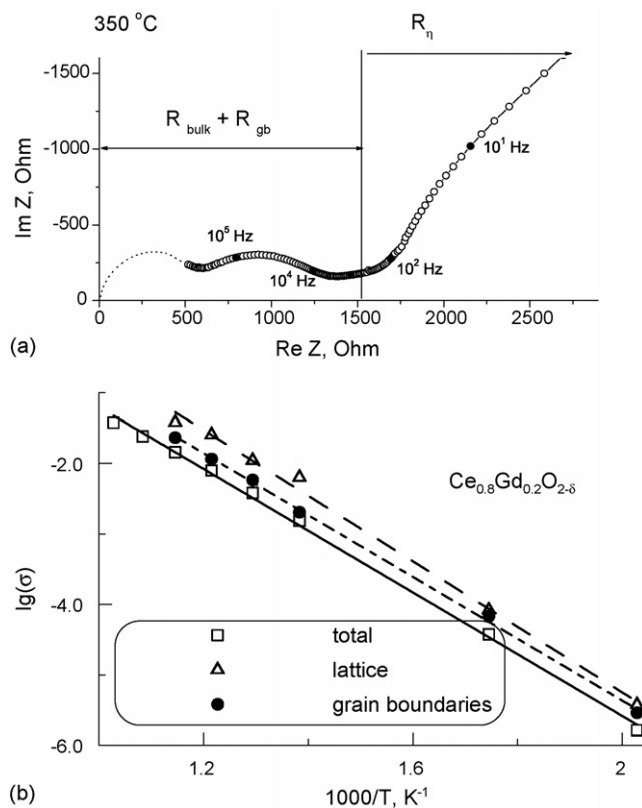


Fig. 6. Example of the impedance spectrum of a Ag/electrolyte/Ag cell at 350 °C (a) and total electroconductivity in comparison with contributions of the grain bulk and grain boundaries conductivities (b).



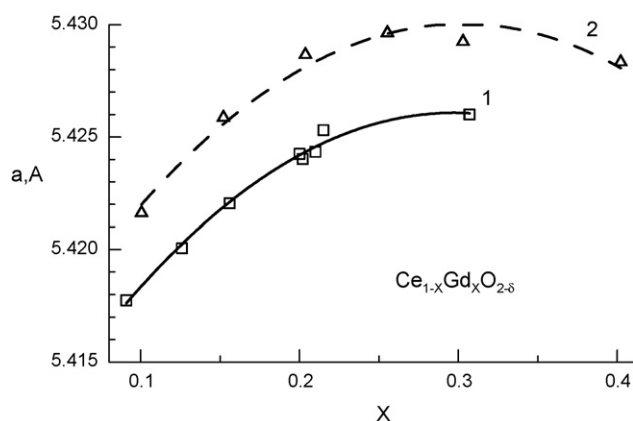


Fig. 7. The influence of the composition of solid electrolytes  $\text{Ce}_{1-x}\text{Gd}_x\text{O}_{2-\delta}$  ( $x=0.09\text{--}0.31$ ) on a lattice parameter: (1) present work and (2) published.<sup>3</sup>

ders, was very large, their contribution to the decrease in the total electroconductivity of the ceramic was insignificant. The bulk electroconductivity of the electrolyte grains in our material was sufficiently high.

We investigated the influence of the composition of sintered solid electrolytes  $\text{Ce}_{1-x}\text{Gd}_x\text{O}_{2-\delta}$  ( $x=0.09\text{--}0.31$ ) on electroconductivity and lattice parameter. The samples with maximum densities, no less than 99%, were selected to maximally reduce the effect of the ceramics' density on the regularities under investigation. The significant deviation to the lower values in lattice parameter of elementary cubic cell for sintered ceramics as compared with the known data for conventional coarse-grained material<sup>3</sup> was revealed (Fig. 7).

The temperature dependences of the electroconductivity were approximated with straight lines in the Arrhenius coordinates that are traditionally used when analyzing thermally activated conduction. Fig. 8 compares the data on the dependence of the effective activation energy for conduction on the concentration of the dopant for the samples of ceramics, which were investigated in this work and which are characterized by an average size of grains on the order of 300 nm, with similar data borrowed from relevant literature<sup>1,3</sup> for ceramics with a micron scale of grains. The absence of a minimum in this dependence makes

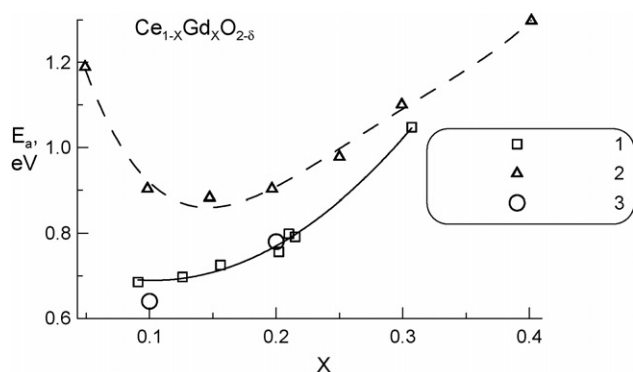


Fig. 8. Dependence of the effective activation energy for electroconduction in solid electrolytes on the basis of  $\text{CeO}_2$  with a submicron scale of the microstructure on the content of the dopant as compared with coarse-grained electrolytes: (1) present work, (2) published<sup>3</sup> and (3) published.<sup>1</sup>

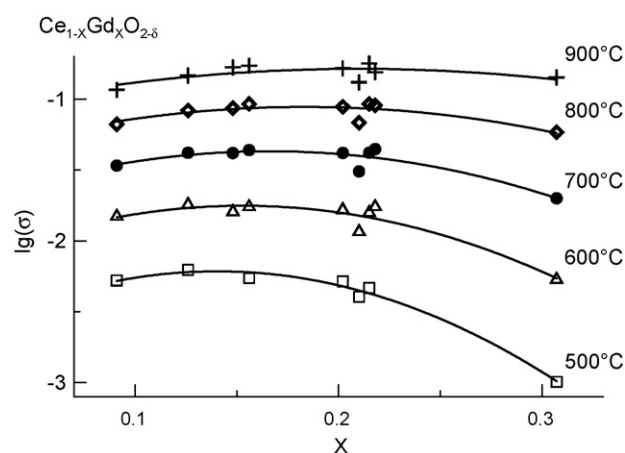


Fig. 9. Isotherms of electroconductivity (in air) for prepared solid electrolytes  $\text{Ce}_{1-x}\text{Gd}_x\text{O}_{2-\delta}$  ( $x=0.09\text{--}0.31$ ) for the temperatures from 900 to 500 °C.

these data substantially different from the data<sup>3</sup> that are characterized by the presence of a minimum. Another distinguishing feature is the smaller value of the effective activation energy for conduction in the obtained solid electrolytes in the range of the gadolinium concentrations studied. The data of another work<sup>1</sup> taken with micron-sized grain ceramics of high purity is in a good agreement with our measurements. This is a good additional evidence for the essential influence of purity of grain boundaries in ceria-based ceramics on total ion conductivity.

In Fig. 9 the data on the electroconductivity of electrolytes with a submicron dimension of grains, are plotted in the form of isotherms for different temperatures as a function of the molar fraction of gadolinium. The electroconductivity isotherms (when plotted in the semilogarithmic coordinates) possess the form of curves with a gently sloping maximum, which shifts, following an increase in the temperature, in the direction of larger concentrations of gadolinium, which contradicts the data reported in.<sup>3</sup> We clearly discern that the maximum electroconductivity at a temperature of 500 °C corresponds to a molar content of gadolinium equal to 0.15, at 800 °C the maximum shifts to  $x=0.21$ . The maximum in the electroconductivity isotherms for the coarse-grained ceramic studied by the authors of<sup>3</sup> does not shift.

#### 4. Conclusions

1. Utilizing nano-sized powders makes it possible to reduce the temperature of the sintering of solid electrolytes  $\text{Ce}_{1-x}\text{Gd}_x\text{O}_{2-\delta}$  ( $x=0.09\text{--}0.31$ ) to 1100–1300 °C and manufacture a ceramic with a submicron (0.1–0.3  $\mu\text{m}$ ) dimension of grains, which exhibits a high electroconductivity.
2. Depending on the molar content of gadolinium, the electroconductivity isotherms for  $\text{Ce}_{1-x}\text{Gd}_x\text{O}_{2-\delta}$  can display a maximum, which shifts in the direction of larger gadolinium contents with increasing temperature.
3. The activation energy for conductivity in solid electrolytes  $\text{Ce}_{1-x}\text{Gd}_x\text{O}_{2-\delta}$  with a submicron size of grains steadily increases with increasing content of gadolinium and in the dopant concentration range studied ( $x=0.09\text{--}0.31$ ).

4. The effect of density and purity on the conductivity of solid electrolytes  $\text{Ce}_{1-x}\text{Gd}_x\text{O}_{2-\delta}$  is considerably stronger than influence of grain size.

### Acknowledgment

This work was supported by IPP DOE, the International Scientific and Technical Center, project no. 2277p.

### References

1. Steele, B. C. H., Appraisal of  $\text{Ce}_{1-y}\text{Gd}_y\text{O}_{2-y/2}$  electrolytes for IT-SOFC operation at 500 °C. *Solid State Ionics*, 2000, **129**, 95–110.
2. Inaba, H. and Tagawa, H., Ceria-based solid electrolytes. *Solid State Ionics*, 1996, **83**, 1–16.
3. Tianshu, Z., Hing, P., Huang, H. and Kilner, J., Ionic conductivity in the  $\text{CeO}_2\text{--Gd}_2\text{O}_3$  system ( $0.05 \leq \text{Gd/Ce} \leq 0.4$ ) prepared by oxalate coprecipitation. *Solid State Ionics*, 2002, **148**, 567–573.
4. Christie, G. M. and Van Berkel, F. P. F., Microstructure–ionic conductivity relationships in ceria–gadolinia electrolytes. *Solid State Ionics*, 1996, **83**, 17–27.
5. Mogensen, M., Sammes, N. M. and Tompsett, G. A., Physical, chemical and electrochemical properties of pure and doped ceria. *Solid State Ionics*, 2000, **129**, 63–94.
6. Kim, S. and Maier, J., On the conductivity mechanism of nanocrystalline ceria. *J. Electrochem. Soc.*, 2002, **149**(10), J73–J83.
7. Van Herle, J., Horita, T., Kawada, T., Sakai, H., Yokokawa, H. and Dokiya, M., Low temperature fabrication of (Y,Gd,Sm)-doped ceria electrolyte. *Solid State Ionics*, 1996, **86–88**, 1255–1258.
8. Suzuki, T., Kosacki, I. and Anderson, H. U., Microstructure–electrical conductivity relationships in nanocrystalline ceria thin films. *Solid State Ionics*, 2002, **151**, 111–121.
9. Kotov, Yu. A., Osipov, V. V., Ivanov, M. G., Samatov, O. M., Platonov, V. V., Azarkevich, E. I. et al., Properties of oxide nanopowders prepared by target evaporation with a pulse-periodic  $\text{CO}_2$  laser. *Tech. Phys.*, 2002, **47**(11), 1420–1426.
10. Kotov, Yu. A., Osipov, V. V., Samatov, O. M., Ivanov, M. G., Platonov, V. V., Murzakaev, A. M. et al., Properties of powders produced by evaporating  $\text{CeO}_2/\text{Gd}_2\text{O}_3$  targets exposed to pulsed-periodic radiation of a  $\text{CO}_2$  laser. *Tech. Phys.*, 2004, **49**(3), 352–357.
11. Ivanov, V., Paragin, S., Khrustov, V., Medvedev, A. and Shtol's, A., Processing of nanostructured oxide ceramics with magnetic pulsed compaction technique. *Key Eng. Mater.*, 2002, **206–213**, 377–380.